Structural Engineering and Mechanics, Vol. 6, No. 3 (1998) 291-304
DOI: http://dx.doi.org/10.12989/sem.1998.6.3.291

Non-axisymmetric dynamic response of imperfectly bonded buried orthotropic pipelines

J.P. Dwivedi†, B.K. Mishra‡ and P.C. Upadhyay‡†

Department of Mechanical Engineering, Institute of Technology, Banaras Hindu University, VARANASI 221 005, India

Abstract. This paper deals with the non-axisymmetric dynamic response of an imperfectly bonded buried orthotropic pipeline subjected to longitudinal wave (*P*-wave) excitation. An infinite cylindrical shell model, including the rotary inertia and shear deformation effects, has been used for the pipeline. For some cases comparison of axisymmetric and non-axisymmetric responses have also been furnished.

Key words: orthotropic; axisymmetric; buried; dynamic response; imperfect bond; cylindrical shell.

1. Introduction

Dynamic response of buried pipeline/lifeline under seismic excitation has emerged as an important field of research. Earlier researchers concentrated mainly on the pipelines made of isotropic material as most of utility lines were made of cast iron and steel. However, today we find that the reinforced plastic mortar pipes (RPM) have found greater acceptance in utility lines, etc. This has led to the need for anlayzing the dynamic response of pipes made of orthotropic materials. As a result, during the last few years a number of papers by Cole, *et al.* (1979), Singh, *et al.* (1987), Singh, *et al.* (1987), Upadhyay and Mishra (1988) and Upadhyay and Mishra (1988), have appeared on the axisymmetric and non-axisymmetric dynamic/seismic responses of buried orthotropic pipes/shells. In most of these work it has been assumed that the pipe/shell remains perfectly bonded to the surrounding medium (soil). In practice, however, this is never true. Chonan (1981) and Datta, *et al.* (1984) have studied the effect of imperfect bond between the pipe and the surrounding soil on the response of the pipe. But again, their work is also limited to the pipes made of isotropic material only.

Dwivedi and Upadhyay (1989), (1991) have studied the effect of imperfect bond on the dynamic response of buried orthotropic cylindrical shell due to seismic excitation. Both these papers are concerned with the axisymmetric response only. There is no work available discussing the effect of bond imperfection on the non-axisymmetric dynamic response of buried pipes made of orthotropic materials. In work reported by Upadhyay and Mishra (1988), Upadhyay and Mishra (1988), it is shown that in certain cases, depending on the soil condition and the nature of wave excitation, flexural mode response may become even more significant than the axisymmetric mode response. Therefore, in this paper we have attempted to analyze the effect of

† Reader
‡ Reader, Department of Mech. and Ind. Engineering, U.O.R. Roorke, India
‡† Professor

imperfect bond on the non-axisymmetric dynamic response of buried orthotropic pipelines.

An approach similar to Dwivedi and Upadhyay (1989) has been followed wherein a thin layer is assumed between the shell and the surrounding medium (soil) such that this layer possesses the properties of stiffness and damping both. The degree of imperfection of the bond is varied by changing the stiffness and the damping parameters of this layer. It is concluded that, the effect of bond imperfection in non-axisymmetric mode is significant because, in general, the consideration of bond imperfection leads to higher values of shell deformation as compared to the same under perfect bond condition.

2. Formulation of the problem

An infinitely long thick orthotropic cylindrical shell of mean radius R and thickness h, is considered to be buried in a linearly elastic, homogeneous isotropic infinite medium. The shell is being excited by a longitudinal wave (P-wave). A wave of wavelength Λ ($=2\pi/\xi$) is considered to strike the shell at angle ϕ with the axis of the shell. Thus the apparent wave speed c along the shell axis is given by $c = c_1/\cos\phi$. c_1 is the speed of propagation of the longitudinal wave in the infinite medium.

A cylindrical-polar co-ordinate system (r, ϕ, x) is defined such that x coincides with the axis of the shell. In addition, if z is measured normal to the shell middle surface such that

$$z = r - R, \qquad -h/2 \le r \le h/2 \tag{1}$$

the equation governing the non-axisymmetric motion of a cylindrical shell can be written as given by Upadhyay and Mishra (1988),

$$[L]\{U\} + \{P^*\} = \{0\} \tag{2}$$

where $[L]$ is a (5×5) matrix. The elements of the matrix $[L]$ in Eq. (2) are the same as given by Upadhyay and Mishra (1988).

$$\{U\} = [w \;\; v \;\; \psi_\theta \;\; u \;\; \psi_x]^T$$

where w, v and u are the displacement components of the middle surface of the shell in radial, tengential and axial directions respectively, and ψ_θ and ψ_x are the angles of rotaion of a straight line initially normal to the middle surface of the shell in the tangential and axial directions, respectively.

The elements of $\{P^*\}$ are given by

$$P_1^* = (1 + z/R)\sigma_{zz}^*, \; P_2^* = (1 + z/R)\sigma_{z\theta}^*, \; P_3^* = (1 + z/R)\sigma_{z\theta}^*,$$
$$P_4^* = (1 + z/R)\sigma_{zx}^*, \text{ and } P_5^* = z(1 + z/R)\sigma_{zx}^*$$

where σ_{ij}^* denotes stresses with their usual meaning.

For the evaluation of $\{P^*\}$, σ_{ij}^* at the outer surface of the shell (i.e., at $z = +h/2$) are determined in terms of the incident and scattered fields in the surrounding medium. The total displacement field in the surrounding soil is written as

$$u = u^{(i)} + u^{(s)} \tag{3}$$

where superscript i and s represent incident and scattered parts respectively. By solving the wave equation in the surrounding infinite medium, components of the incident and scattered

fields for the nth mode ($n=0$ and $n \neq 0$, correspond to axisymmetric and non-axisymmetric modes, respectively) can be written as

$$u_r^{(i)} = \left[\left\{\gamma I'_n(\gamma\frac{r}{R})\right\}B_1\right]\cos n\theta \exp.[i\xi(x-ct)],$$

$$u_\theta^{(i)} = \left[\left\{-n(R/r)I_n(\gamma\frac{r}{R})\right\}B_1\right]\sin n\theta \exp.[i\xi(x-ct)],$$

$$u_x^{(i)} = \left[\left\{i\beta I_n(\gamma\frac{r}{R})\right\}B_1\right]\cos n\theta \exp.[i\xi(x-ct)] \tag{4}$$

$$u_r^{(s)} = \left[\left\{\gamma K_n'(\gamma\frac{r}{R})\right\}B_2 + \left\{-i\beta\delta K_n'(\delta\frac{r}{R})\right\}B_3 + \left\{n(R/r)K_n(\delta\frac{r}{R})\right\}B_4\right]\cos n\theta \exp.[i\xi(x-ct)],$$

$$u_\theta^{(s)} = \left[\left\{-n(R/r)K_n'(\gamma\frac{r}{R})\right\}B_2 + \left\{-in(R/r)\beta K_n'(\delta\frac{r}{R})\right\}B_3 + \left\{-\delta K_n'(\delta\frac{r}{R})\right\}B_4\right]$$
$$\sin n\theta \exp.[i\xi(x-ct)],$$

$$u_x^{(s)} = \left[\left\{i\beta K_n'(\gamma\frac{r}{R})\right\}B_2 + \left\{\delta^2 K_n'(\delta\frac{r}{R})\right\}B_3\right]\cos n\theta \exp.[i\xi(x-ct)] \tag{5}$$

where I_n and K_n are modified Bessel functions of the first and second kind respectively, and $\beta=\xi R=2\pi R/\Lambda$, $\gamma=(\beta^2-\varepsilon_1^2)^{1/2}$, $\delta=(\beta^2-\varepsilon_2^2)^{1/2}$, $\varepsilon_1=\beta\frac{c}{c_1}=(\beta/\cos\phi)$, $\varepsilon_2=\beta\frac{c}{c_2}$, $c_1=\{(\lambda+2\mu)/\rho_m\}^{1/2}$ and $c_2=(\mu/\rho_m)^{1/2}$ · B_1 depends upon the intensity of incident P-wave and has dimension of length. B_2, B_3 and B_4 are arbitrary constants. (′) denotes differentiation with respect to the arguments of the Bessel functions.

The stresses at the outer surface of the shell (at $r=R+h/2$) can be obtained from the displacement field of the surrounding medium, thus $[P^*]$ can be evaluated. Now the shell displacements are assumed of the form

$$w=w_o\cos n\theta \exp[i\xi(x-ct)],\ v=v_o\sin n\theta \exp[i\xi(x-ct)],$$
$$u=u_o\cos n\theta \exp[i\xi(x-ct)],\ \psi_x=\psi_{xo}\cos n\theta \exp[i\xi(x-ct)], \text{ and} \tag{6}$$
$$\psi_\theta=\psi_{\theta o}\sin n\theta \exp[i\xi(x-ct)]$$

These, along with $\{P^*\}$ are substituted into Eq. (2) to yield a set of five simultaneous equations. Three more equations are obtained by enforcing the boundary conditions at the outer surface of the shell.

Boundary conditions at the outer surface of the shell ($r=R+h/2$) are obtained by assuming that the shell and continuum are joined together by a bond which is thin, elastic and inertialess. This implies that the stresses at the shell-soil interface are continuous. To take the elasticity of the bond into account, the stresses in the bond are assumed proportional to the relative displacements between the shell and continuum, i.e.,

$$\sigma_{rr}\,|_{r=R+h/2}=\left(S_r+Z_r\frac{\partial}{\partial t}\right)\{u_r^i+u_r^s-w\}\,|_{r=R+h/2}$$

$$\sigma_{r\theta}|_{r=R+h/2}=\left(S_\theta+Z_\theta\frac{\partial}{\partial t}\right)\{u_\theta^i+u_\theta^s-u-(r-R)\psi_\theta\}\,|_{r=R+h/2}$$

$$\sigma_{rx}\,|_{r=R+h/2}=\left(S_x+Z_x\frac{\partial}{\partial t}\right)\{u_x^i+u_x^s-u-(r-R)\psi_x\}\,|_{r=R+h/2} \tag{7}$$

where S_r, S_θ and S_x are the stiffness coefficients of the bond in radial, tangential and axial directions, respectively. Z_r, Z_θ and Z_x are the damping coefficients of the bond in radial, tangential and axial directions, respectively.

Eqs. (2) and (7) yield together a set of eight algebraic equations which when simplified, give the final response equation as

$$[Q\,]\{\bar{U}_0\}=\{F^1\} \tag{8}$$

where $[Q]$ is a (8×8) matrix and $\{F^1\}$ is (8×1) matrix. All the elements of the Q_{ij} matrices remain same as given by Upadhyay and Mishra (1988) except Q_{ij} with $i, j = 6, 7$ and 8 for which the expressions are as follows:

$$Q_{66}=-\gamma K_n'(\alpha_1)+\frac{\zeta_r\Gamma_r}{\Gamma_r-i\varepsilon_1\zeta_r}[(2\varepsilon_1^2-\varepsilon_2^2)K_n(\alpha_1)+2\gamma K_n''(\alpha_1)]\,,$$

$$Q_{67}=i\beta\delta K_n'(\alpha_2)-\frac{\zeta_r\Gamma_r}{\Gamma_r-i\varepsilon_1\zeta_r}[2i\beta\delta^2K_n''(\alpha_2)]\,,$$

$$Q_{68}=\{-nK_n(\alpha_2)/(1+\bar{h}/2)\}+\frac{\zeta_r\Gamma_r}{\Gamma_r-i\varepsilon_1\zeta_r}[2n\{\alpha_2K_n'(\alpha_2)-K_n(\alpha_2)\}/(1+\bar{h}/2)]\,,$$

$$Q_{76}=\{nK_n(\alpha_1)/(1+\bar{h}/2)\}+\frac{\zeta_\theta\Gamma_\theta}{\Gamma_\theta-i\varepsilon_1\zeta_\theta}[2n\{K_n(\alpha_1)-\alpha_1K_n'(\alpha_1)\}/(1+\bar{h}/2)^2]\,,$$

$$Q_{77}=\{-in\beta K_n(\alpha_2)/(1+\bar{h}/2)\}+\frac{\zeta_\theta\Gamma_\theta}{\Gamma_\theta-i\varepsilon_1\zeta_\theta}[2in\beta\{\alpha_2K_n'(\alpha_2)-K_n(\alpha_2)\}/(1+\bar{h}/2)^2]\,,$$

$$Q_{78}=\delta K_n'(\alpha_2)+\frac{\zeta_\theta\Gamma_\theta}{\Gamma_\theta-i\varepsilon_1\zeta_\theta}[\{-\delta^2K_n''(\alpha_2)+\delta^2K_n'(\alpha_2)/(1+\bar{h}/2)-n^2K_n(\alpha_2)\}/(1+\bar{h}/2)^2],$$

$$Q_{86}=-i\beta K_n(\alpha_1)+\frac{\zeta_x\Gamma_x}{\Gamma_x-i\varepsilon_1\zeta_x}[2i\beta K_n'(\alpha_1)]\,,$$

$$Q_{87}=-\delta^2K_n(\alpha_2)+\frac{\zeta_x\Gamma_x}{\Gamma_x-i\varepsilon_1\zeta_x}[\delta(2\beta^2-\varepsilon_2^2)K_n'(\alpha_2)]\,,$$

$$Q_{88}=\frac{\zeta_x\Gamma_x}{\Gamma_x-i\varepsilon_1\zeta_x}[in\beta K_n(\alpha_2)/(1+\bar{h}/2)].$$

Similarly, the components of F_j^1 also remain same as given Upadhyay and Mishra (1988) except F_j^1 with $j = 6, 7$ and 8 which are given as:

$$F_6^1=\gamma I_n'(\alpha_2)-\frac{\zeta_r\Gamma_r}{\Gamma_r-i\varepsilon_1\zeta_r}[(2\varepsilon_1^2-\varepsilon_2^2)I_n(\alpha_1)+2\gamma^2I_n''(\alpha_1)]$$

$$F_7^1 = -\{nI_n(\alpha_1)/(1+\bar{h}/2)\} - \frac{\zeta_\theta \Gamma_\theta}{\Gamma_\theta - i\varepsilon_1\zeta_\theta}[2n\{I_n(\alpha_1) - \alpha_1 I_n'(\alpha_1)\}/(1+\bar{h}/2)^2],$$

$$F_8^1 = i\beta I_n(\alpha_1) - \frac{\zeta_x \Gamma_x}{\Gamma_x - i\varepsilon_1\zeta_x}[2i\beta\gamma I_n'(\alpha_1)],$$

The response vector $\{\bar{U}_o\}$ in Eq. (8) is given as

$$\{\bar{U}\} = \left[\bar{W}\ \bar{V}\ (h\psi_{\theta o}/2B_1)\bar{U}\ (h\psi_{\theta o}/2B_1)\frac{B_2}{B_1}\ \frac{B_3}{B_1}\ \frac{B_4}{B_1}\right]^T$$

where $\bar{W} = (w_o/B_1)$, $\bar{V} = (v_o/B_1)$ and $\bar{U} = (u_o/B_1)$ are the non-dimensional deformation amplitudes of the shell middle surface in radial, tangential and axial directions respectively.

Different parameters and material constants occuring in above equations are as followings:

$$\bar{h} = h/R,\ \eta_1 = \frac{E_\theta}{E_x},\ \eta_2 = \frac{G_{xz}}{E_x},\ \eta_3 = \frac{G_{x\theta}}{E_x},\ \eta_4 = \frac{G_{z\theta}}{E_x},\ N = \frac{1}{(1-\nu_{x\theta}\nu_{\theta x})},\ \bar{\mu} = \mu/G_{xz}$$

$$\Omega^2 = \rho h\omega^2 R/G_{xz} = \bar{h}\bar{\mu}\varepsilon_2^2/\bar{\rho},\ \bar{\rho} = \rho_m/\rho,\ \alpha_1 = (1+\bar{h}/2)\gamma,\ \alpha_2(1+\bar{h}/2)\delta$$

μ and ρ_m are the shear modulus and density of the medium, respectively amd ρ is the density of the shell material.

$\zeta_r = \frac{\mu}{S_r R}$, $\zeta_\theta = \frac{\mu}{S_\theta R}$ and $\zeta_x = \frac{\mu}{S_x R}$ are the non-dimensionalized stiffness coefficients of the bond in radial, tangential and axial direction respectively. $\Gamma_r = \frac{\mu}{Z_r c_1}$, $\Gamma_\theta = \frac{\mu}{Z_\theta c_1}$ and $\Gamma_x = \frac{\mu}{Z_x c_1}$ are the non-dimensionalized damping coeffcients of the bond in radial, tangential and axial direction respectively.

3. Results and discussion

Results have been presented here for a transversely isotropic shell with r-θ as the plane of isotropy. This makes

$E_\theta = E_z$, $G_{xz} = G_{x\theta}$, $\nu_{x\theta} = \nu_{z\theta}$, $\nu_{x\theta} = \nu_{xz}$ and $G_{z\theta} = \frac{E_\theta}{2(1+\nu_{\theta z})}$, and consequently $\eta_2 = \eta_3$ and $\eta_4 = \frac{G_{z\theta}}{E_x} = \frac{\eta_1}{2(1+\nu_{\theta z})}$. Further, $\nu_{x\theta} = \nu_{z\theta} = \nu_{xz}$ has been taken as 0.3.

Effects of imperfect bond between the shell and the surrounding soil has been shown by furnishing the response ($\bar{U}$, $\bar{V}$ & $\bar{W}$) plots against the wavelength parameter β, taking the stiffness (ζ_x, ζ_θ, ζ_r) and the damping coefficients (Γ_x, Γ_θ, Γ_r) of the bond as parameters. The bond parameters have been varied between zero and infinity. $\zeta_X = \zeta_\theta = \zeta_r = \Gamma_x = \Gamma_\theta = \Gamma_r = 0$ corresponds to a perfect bonding between the shell and surrounding soil. Therefore, while depicting the effect of one particular bond parameter, others are kept constant at zero value. Effects of soil condition and the angle of wave incidence have also been discussed by varying parameters $\bar{\mu}$ and ϕ, respectively. $\bar{\mu}$ has been taken as 0.01, 0.10 and 1.0. The value of $\bar{\mu} = 0.01$ represents a soft and sandy ground conditions whereas $\bar{\mu} = 1.0$ or more represents a hard and

rocky surrounding. For $\bar{\mu}=0.01$, v_m has been taken to be 0.45 and for higher value of $\bar{\mu}$, $v_m=0.25$ has been used.

The angle of wave incidence have been selected as 5°, 60° and 80°. $\phi=5°$ represents nearly an grazing angle of incidence, whereas 60° represents a general striking angle of incidence wave. Since, a detailed discussion on the effects of variation of orthotropy parameters (η_1 and η_2) has already been reported by Upadhyay and Mishra (1988), therefore, their effects have not been shown in this study and hence $\eta_1=0.1$ and $\eta_2=0.5$ has been kept constant throughout the discussion. Other values taken constant are:
$\bar{h}=0.05$ and $\bar{\rho}=0.75$

Fig. 1 shows the relative contributions of different modes on the axial displacement, $\bar{U}$, with axial bond stiffness ζ_x as parameter, for $\bar{\mu}=0.1$ and $\phi=60°$. It is observed that the magnitude of axisymmetric mode response can go even higher than that of the non-axisymmetric response when shell is perfectly bonded to the surrounding medium. The difference in response of two modes is visual for any range of wavelength, however, it is more prominant when β approaches 0.5. Under imperfect bond condition ($\zeta_x=10^2$) axial displacement ($\bar{U}$) in non-axisymmetric mode is found to be almost comparable to axisymmetric mode response at smaller value of β, but at shorter wavelength ($\beta>0.5$) the non-axisymmetric mode shows a higher value of $\bar{U}$. It is observed that the magnitude of axial displacement is always higer when there is perfect bond between shell and the soil. In $n=2$ mode, bond imperfection does not appear to have any appreciable effect because the contribution of this mode itself is very impressive. Same pattern of results were observed when the contribution of different modes on the radial displacement, $\bar{W}$, and the tangential displacement ($n>0$ only), $\bar{V}$, was plotted taking ζ_r and ζ_θ as parameters, respectively. As Upadhyay and Mishra (1988), Upadhyay and Mishra (1988), has concluded in their papers, it is realized that the flexural mode response cannot be ignored whether there be a perfect bond or imperfect bond between the pipe and the surrounding soil (medium).

Since the comparison of axisymmetric and flexural mode for a perfectly bonded case by

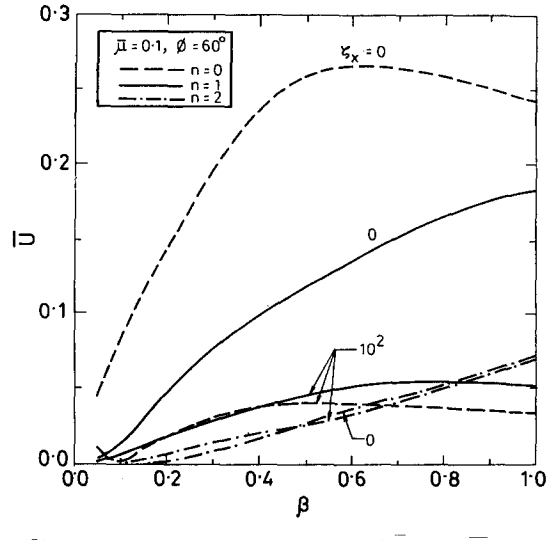

Fig. 1 Wavelength parameter (β) versus Axial displacement ($\bar{U}$) for $\bar{\mu}=0.1$, $\phi=60°$ with ζ_x and n as parameters.

Upadhyay and Mishra (1988), and the effects of imperfect bond in case of axisymmetric mode have already been reported by Dwivedi and Upadhyay (1989), only the flexural mode ($n = 1$) response for imperfectly bonded shell is being presented here in rest of the plots.

Figs. 2-5 show the effect of variation of axial stiffness parameter (ζ_x) of the bond on the axial displacement ($\bar{U}$) of the shell under different soil conditions and wave incidence angles. It is seen that beyond $\zeta_x = 10^2$ changes in ζ_x no longer change $\bar{U}$ values. Therefore, for all practical purposes, a value of ζ_x greater than 10^2 can be considered as equivalent to $\zeta_x = \infty$.

Figs. 2 and 3 show the variation of $\bar{U}$ against β under a soft soil condition ($\bar{\mu} = 0.01$) for $\phi =$ 5° & 60°, respectively. At grazing angle of incidence (Fig. 2), $\bar{U}$ is seen to be increaseing as ζ_x

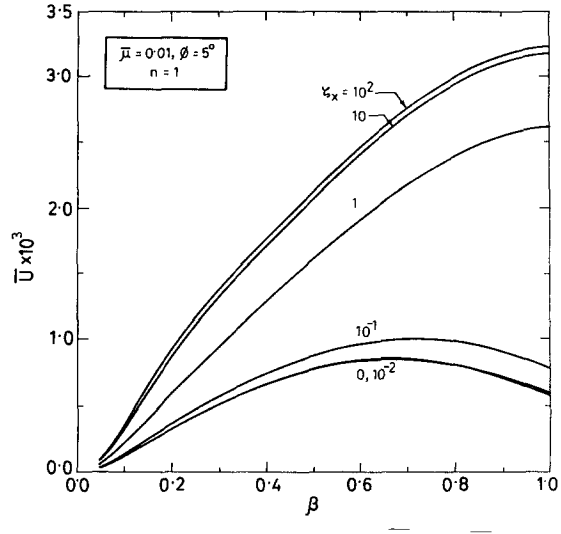

Fig. 2 Wavelength parameter (β) versus Axial displacement ($\bar{U}$) for $\bar{\mu} = 0.01$, $\phi = 5°$ and $n = 1$ with ζ_x as parameter.

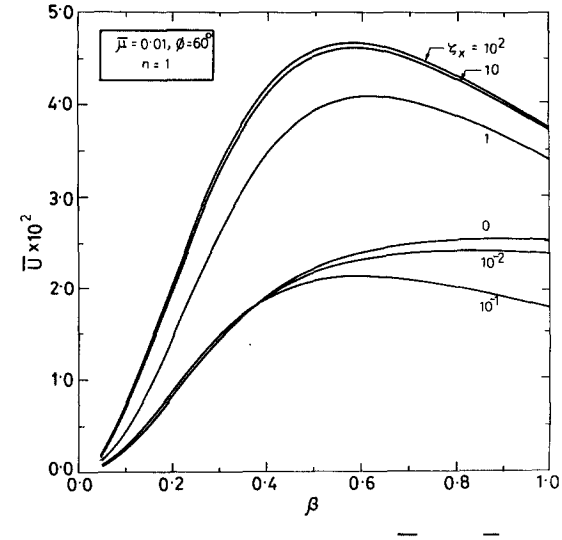

Fig. 3. Wavelength parameter (β) versus Axial displacement ($\bar{U}$) for $\bar{\mu} = 0.01$, $\phi = 60°$ and $n = 1$ with ζ_x as parameter.

is increased (bond becomes loose). But at an increased angle of incidence (at $\phi = 60^\circ$) in Fig. 3, a different trend is observed. Here axial displacement ($\bar{U}$) first decreases with increase in ζ_x up to 10^{-1}. But as ζ_x is increased further, $\bar{U}$ goes much higher than the one for perfectly bonded shell ($\zeta_x = 0$). At $\zeta_x = 10$ or 10^2 the value of $\bar{U}$ becomes nearly double the value for perfectly bonded case. At higher angles of incidence ($\phi = 80^\circ$) and with same soil condition, the trend was similar to that observed for $\phi = 60^\circ$.

In Fig. 4, $\bar{U}$ vs. β plots are given for $\phi = 5^\circ$ and $\bar{\mu} = 0.1$. A comparison between Figs. 2 and 4 shows the effect of increasing the soil rigidity when ϕ is 5°. As soil rigidity is increased from 0.01 to 0.1, for same angle of incidence ($\phi = 5^\circ$), a reversed trend is observed

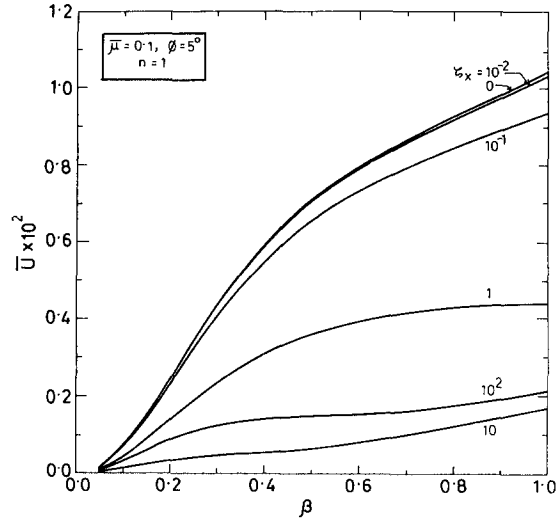

Fig. 4 Wavelength parameter (β) versus Axial displacement ($\bar{U}$) for $\bar{\mu} = 0.1$, $\phi = 5^\circ$ and $n = 1$ with ζ_x as parameter.

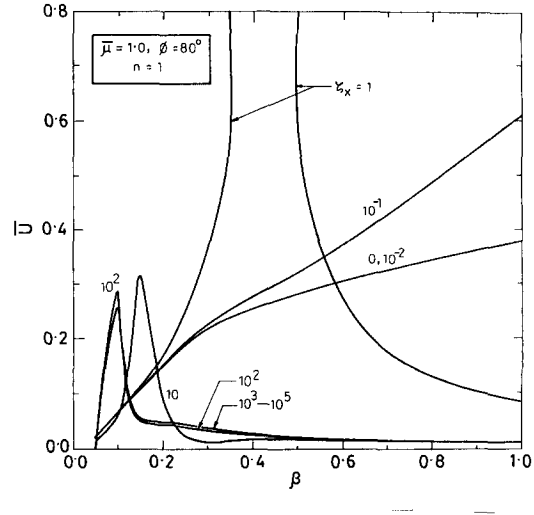

Fig. 5 Wavelength parameter (β) versus Axial displacement ($\bar{U}$) for $\bar{\mu} = 1.0$, $\phi = 80^\circ$ and $n = 1$ with ζ_x as parameter.

in Fig. 4. It is observed that with an imperfect bond condition $\bar{U}$ is now smaller than it is for a perfect bond condition. Thus Figs. 2 and 4 clearly bring out the effect of soil rigidity for imperfectly bonded pipes. Although not shown but similar pattern is observed at higher angle of incidence($\phi = 80^\circ$).

When $\bar{\mu}$ and ϕ both are increased to $\bar{\mu} = 0.1$ and $\phi = 80^\circ$, $\bar{U}$ vs. β plots are shown in Fig. 5. The location and the intensity of peaks are seen to be dependent on the value of ζ_x. Figure shows that in moderately hard soil ($\bar{\mu} = 0.1$) with angle of incidence $\phi = 80^\circ$, peaks are observed in $\bar{U}$ plot. It is seen that locations of the peaks shift towards lower β and the intensity of the peaks decreases with increase in bond imperfection (ζ_x). The effect of variation in the axial bond

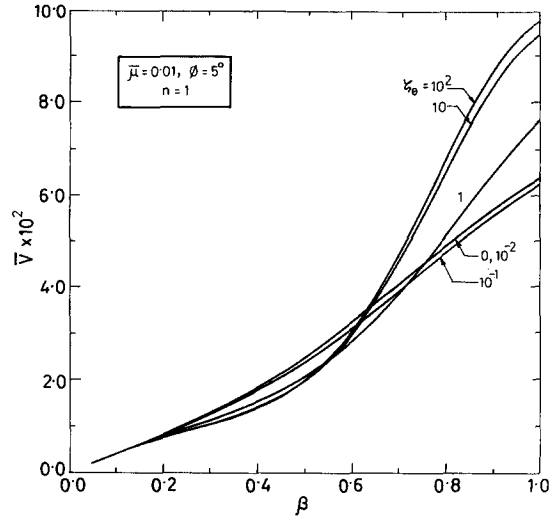

Fig. 6 Wavelength parameter (β) versus Tangential displacement ($\bar{V}$) for $\bar{\mu} = 0.01$, $\phi = 5^\circ$ and $n = 1$ with ζ_θ as parameter.

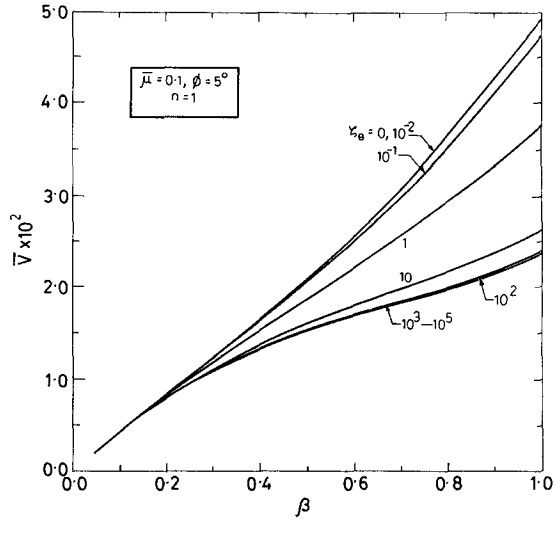

Fig. 7 Wavelength parameter (β) versus Tangential displacement ($\bar{V}$) for $\bar{\mu} = 0.1$, $\phi = 5^\circ$ and $n = 1$ with ζ_θ as parameter.

stiffness (ζ_x) on the tangential and radial displacements ($\bar{V}$ & $\bar{W}$) was not found to be any significance.

In Figs. 6 and 7 are shown the effects of the tangential stiffness coefficient of the bond (ζ_θ) on the tangential displacement $\bar{V}$ of the shell. In soft and sandy soil ($\bar{\mu} = 0.1$) for $\phi = 5^\circ$ $\bar{V}$ increased as ζ_θ is increased, as shown in Fig. 6. However, this trend is prominent only when $\beta > 0.65$, otherwise displacement closely follows each other in the range of β from 0.2 to 0.65. As soil is made little harder ($\bar{\mu} = 0.1$) and ϕ remains unchanged, an reverse trend is oberved. It is observed from Fig. 7 that $\bar{V}$ goes on decreasing as the perfect bond condition is relaxed and ζ_θ is increased. When $\bar{\mu}$ is increased to 1.0 and ϕ is raised to 80°, the nature of variation of $\bar{V}$ is shown in Fig. 8. $\bar{V}$ increases as ζ_θ is increased and attains a sharp peak

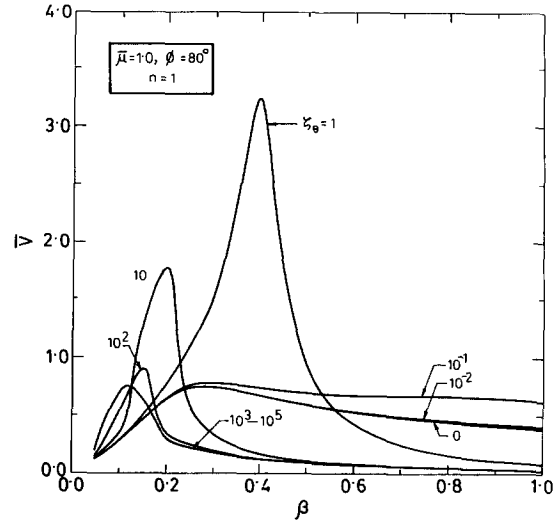

Fig. 8 Wavelength parameter (β) versus Tangential displacement ($\bar{V}$) for $\bar{\mu} = 1.0$, $\phi = 80^\circ$ and $n = 1$ with ζ_θ as parameter.

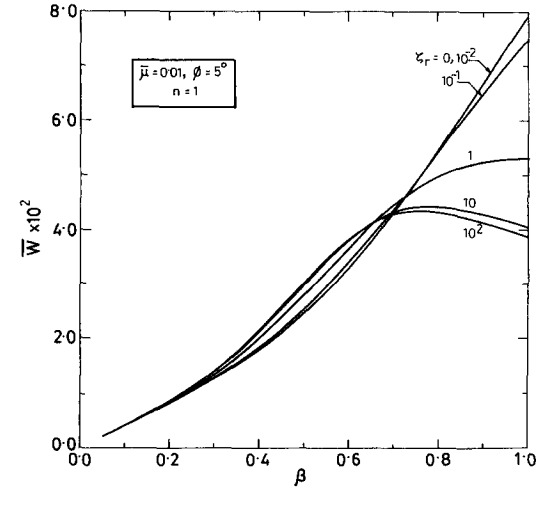

Fig. 9 Wavelength parameter (β) versus Radial displacement ($\bar{W}$) for $\bar{\mu} = 0.01$, $\phi = 5^\circ$ and $n = 1$ with ζ_r as parameter.

at $\zeta_\theta = 1$. With increasing ζ_θ, these peaks appear to be shifting to the left, as was the case with axial displacement in Fig. 5.

In Fig. 9 is shown the effect of variation of the radial stiffness coefficient (ζ_r) of the bond on the radial displacement ($\bar{W}$). Figure shows that for $\bar{\mu} = 0.1$ and at grazing angle of inidence ($\phi = 5^\circ$) $\bar{W}$ increaes as ζ_r is decreased, as β approaches 1. However, in a particular range of wavelength ($0.2 < \beta < 0.65$) this trend has reversed although difference in $\bar{W}$ is not so prominent. As $\bar{\mu}$ is increased to 0.1 and ϕ to 60° (i.e., Fig. 10) radial displacement increases with increase in bond parameter ζ_r. The difference in $\bar{W}$ with increasing value of ζ_r appears to be large as β approach unity. Plot in Fig. 11 for $\bar{\mu} = 0.1$ and $\phi = 80^\circ$ describes the same nature of variation of

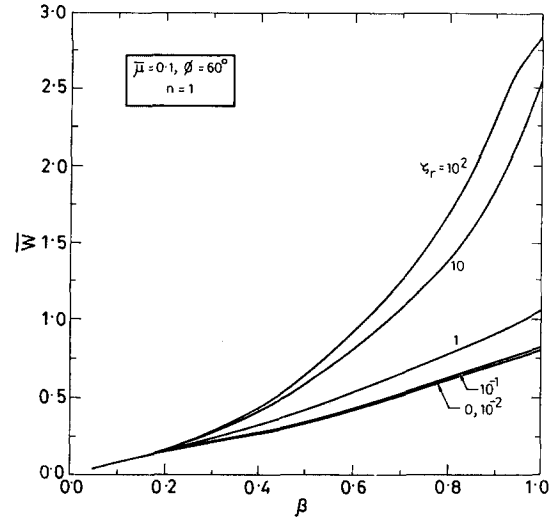

Fig. 10 Wavelength parameter (β) versus Radial displacement ($\bar{W}$) for $\bar{\mu} = 0.1$, $\phi = 60^\circ$ and $n = 1$ with ζ_r as parameter.

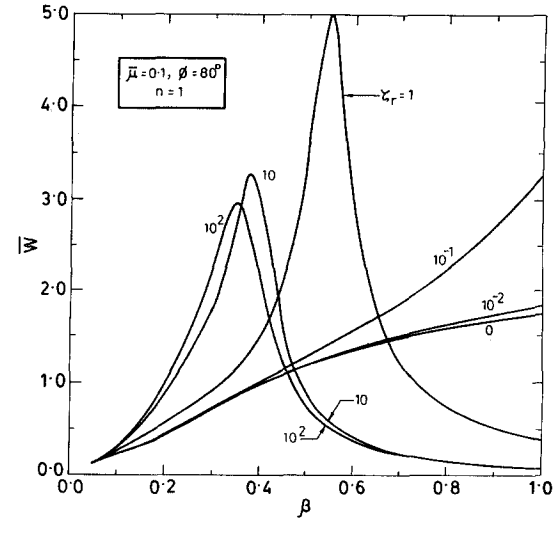

Fig. 11 Wavelength parameter (β) versus Radial displacement ($\bar{W}$) for $\bar{\mu} = 0.1$, $\phi = 80^\circ$ and $n = 1$ with ζ_r as parameter.

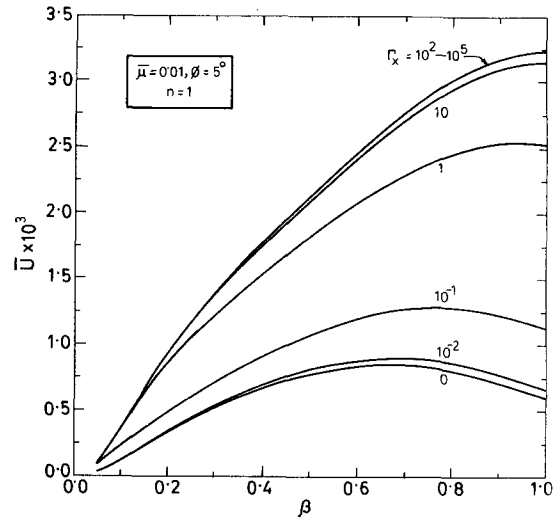

Fig. 12 Wavelength parameter (β) versus Axial displacement ($\bar{U}$) for $\bar{\mu}=0.01$, $\phi=5^\circ$ and $n=1$ with Γ_x as parameters.

$\bar{W}$ as discussed for $\bar{V}$ in Fig. 8. The effect of the axial damping parameter, Γ_x *on* $\bar{U}$ is shown in Fig. 12. The changes in $\bar{U}$ due to variation of Γ_x is identical to that shown for the variation of ζ_x, in Fig. 1. It has also been observed that the bond stiffness of a particular direction affects the displacement component of that direction only. That is, ζ_x, ζ_θ and ζ_r affect only the axial, tangential and the radial components of the displacemtnt, respectively.

4. Conclusions

On the basis of the results presented, the following conclusions can be drawn:

1) Unlike the behaviour observed in axisymmetric mode by Dwivedi and Upadhyay (1989), a loose contact between the shell and the surrounding soil does not always give lower shell displacements as compared to the same for a perfectly bonded shell. Therefore, assumption of a perfect bond may not always lead to a safe and conservative estimate of the shell displacements and, hence, consideration of the bond imperfection in non-axisymmetric mode response is necessary.

2) Effects of bond parameters depend upon the soil condition, incidence angle and the wavelength of the incident wave. In hard surrounding soil and at higher angle of wave incidence bond imperfection has very strong influence on the shell response.

3) Non-axisymmetric response of imperfectly bonded shell is of considerable importanc. Effect of bond imperfection on the axial deformation is of great significance for the axisymmetric as well as the flexural mode ($n=1$). It is observed that the axial deformation of perfectly bonded shell in axisymmetric mode is much more than the same in non-axisymmetric mode; however, they become comparable when an imperfect bond is considered.

4) Bond imperfection taken in a particular direction affects the shell deformation mainly in that direction. It gives very little effect on the deformations in other directions.

References

Chonan, S. (1981). "Dynamic response of a cylindrical shell imperfectly bonded to a surrounding continuum of infinite extent", *Journal of Sound and Vibration,* **78,** 257-267.

Cole, B.W., Ritter, C.J. and Jordan,. (1979), "Structural analysis of buried reinforced mortar pipe", *Lifeline Earthquake Engineering-Buried Pipelines, Seismic Risk and Instrumentation*, T. Ariman, S.C. Liu, and R.E. Nickell, eds., *ASME.*

Datta, S.K. Chakraborty T., and Shah, A.H. (1984). "Dynamic response of pipelines to moving load", *Earthquake Engineering and Structural Dynamics,* **12**, 59-72.

Dwivedi, J.P., and Upadhyay, P.C. (1989). "Effect of imperfect bonding on the axisymmetric dynamic response of buried orthotropic cylindrical shells", *Journal of Sound and Vibration,* **135**(3), 477-486.

Dwivedi, J.P., and Upadhyay, P.C. (1991). "Effect of imperfect bonding on the dynamic response of buried orthotropic cylindrical shells under shear-wave excitaion", *Journal of Sound and Vibration,* **145**(2), 333-337.

Singh, V.P., Upadhyay, P.C., and Kishore, B. (1987), "On the dynamic response of buried orthotropic cylindrical shells", *Journal of Sound and Vibration,* **113**, 101-115.

Singh, V.P., Upadhyay, P.C., and Kishore, B. (1987), "A comparison of thick and thin shell theory results of buried orthotropic cylindrical shells", *Journal of Sound and Vibration,* **119**, 339-345.

Upadhyay, P.C., and Mishra, B.K. (1988). "Non-axisymmetric dynamic response of buried orthotropic cylindrical shells", *Journal of Sound and Vibration,* **121**, 149-160.

Upadhyay, P.C., and Mishra, B.K. (1988). "Non-axisymmetric dynamic response of buried orthotropic cylindrical shells due to incident shear waves", *Journal of Sound and Vibration,* **121**(2), 227-239.

Notations

c	apparent wave speed along the axis of the shell
c_1	speed of dilational wave in the medium
c_2	speed of shear wave in the medium
E_x, E_z, E_θ	Young's moduli of the shell
$G_{x\theta}$, G_{xz}, $G_{z\theta}$	shear moduli of the shell
$\bar{h}$	non-dimensional thickness of the shell
R	mean radius of the shell
S_r, S_x, S_θ	stiffness coefficients of the bond in the radial, axial and tangential directions, respectively
u	displacement of the shell middle surface in axial direction
u_o	displacement amplitude of the shell middle surface in axial direction
u_r, u_x, u_θ	components of displacement vector u
v	displacement of the shell middle surface in the tangential direction
v_o	displacement amplitude of the shell middle surface in the tangential direction
w	displacement of the shell middle surface in the radial direction
w_o	displacement amplitude of the shell middle surface in the radial direction
Z_r, Z_x, Z_θ	damping coefficients of the bond in the bond in the radial, axial and tangential direction, respectively
β	non-dimentional wavenumber of incident wave
Γ_r, Γ_x, Γ_θ	non-dimentional damping coefficient of the bond in the radial, axial and tangential directions, respectively
ζ_r, ζ_x, ζ_θ	non-dimentional stiffness coefficient of the bond in the radial, axial and tangential directions, respectively
η_1, η_2, η_3, η_4	non-dimensional orthropy parameters of the shell

Λ	wavelength of the incident wave
λ	Lame's constant
μ	Lame's constant
$\overline{\mu}$	non-dimensional modulus of rigidity of the medium
ν_m	poissons ratio of the medium
$\nu_{n\theta}, \nu_{\theta x}, \nu_{\theta z}, \nu_{z\theta}, \nu_{zx}, \nu_{xz}$	poissons ratio of the shell
ξ	apparent wavenumber
ρ	density of the shell material
ρ_m	density of the medium
$\overline{\rho}$	non-dimensional density of the medium
σ_{ij}	components of stress tensor
ϕ	angle of wave incidence
ψ_x	angle of rotation, in *r-x* plane, of a line initially normal to midsurface of the shell
ψ_{xo}	amplitude of ψ_x
ψ_θ	angle of rotation, in r-θ plane, of a line initially normal to midsurface of the shell
$\psi_{\theta o}$	amplitude of ψ_θ

Subscripts

m	medium
r	radial direction
x	axial direction
z	normal to middle surface of the shell
θ	tangential direction

Superscripts

i	incident field
s	scattered field